Kinetic study of the selective hydrogenation of styrene over a Pd egg-shell composite catalyst

Carolina Betti[a], Juan Badano[a], Cecilia Lederhos[a], María Maccarrone[a], Nicolás Carrara[a], Fernando Coloma-Pascual[b], Mónica Quiroga[a,c] & Carlos Vera[*,a,c]

[a] Instituto de Investigaciones en Catálisis y Petroquímica INCAPE, FIQ, UNL-CONICET), Predio CCT CONICET Santa Fe, Colectora Ruta Nac. N° 168 Km 0 - Paraje El Pozo, (3000) Santa Fe, Argentina.
[b] Servicios Técnicos de Investigación, Facultad de Ciencias, Universidad de Alicante, Apartado 99, E-03080 Alicante, Spain.
[c] Facultad de Ingeniería Química, Universidad Nacional del Litoral, Santiago del Estero 2829, S3000AOJ, Santa Fe.

Abstract This is a study on the kinetics of the liquid-phase hydrogenation of styrene to ethylbenzene over a catalyst of palladium supported on an inorganic-organic composite. This support has a better mechanical resistance than other commercial supports, e.g. alumina, and yields catalysts with egg-shell structure and a very thin active Pd layer. Catalytic tests were carried out in a batch reactor by varying temperature, total pressure and styrene initial concentration between 353-393 K, 10-30 bar, and 0.26-0.60 mol L^{-1}, respectively. Kinetic models were developed on the assumptions of dissociative hydrogen chemisorption and non-negligible adsorption of hydrogen and styrene. Final chemical reaction expressions useful for reactor design were obtained. The models that best fitted the experimental data were those ones that considered the surface reaction as the limiting step. In this sense a two-step Horiuti-Polanyi working mechanism with half hydrogenation intermediates gave the best fit of the experimental data. The heats of adsorption of styrene and ethylbenzene were also estimated.

Keywords Selective hydrogenation · Styrene · Palladium · Composite · Kinetics

Introduction

Selective hydrogenations are an important class of reactions both from scientific and industrial point of view. Important industrial applications are the purification of refinery streams, the synthesis of chemical intermediates and the synthesis of fine chemicals [1, 2]. From the scientific point of view selective hydrogenations are difficult reactions where selectivity has a great importance because there are usually several degrees of hydrogenation for one same bond or molecules with different functional groups but only one of them needs to be hydrogenated.

One important industrial application is the partial hydrogenation of highly reactive unstable compounds contained in refinery streams coming from cracking or pyrolysis of heavy cuts. Pyrolysis gasoline (PYGAS) is normally produced in ethylene plants processing butane, naphtha or gasoil. PYGAS is a product in the naphtha boiling range, with carbon numbers between C_5-C_{11}, with a high content of aromatics and olefins. It is used for blending with gasoline or as a raw material for the extraction of benzene, toluene and xylene (BTX) [3]. In this context, due to the increasing world trend towards the processing of heavier and cheaper raw materials for the generation of light olefins, the problem arises of finding use for growing stocks of PYGAS. Generally speaking the average composition of PYGAS is 8-12% paraffins, 58-62% aromatics, 8-10% olefins, 18-22% diolefins and 50-300 ppm sulfur, possibly containing higher or lower sulfur amounts and other heteroatoms depending on the origin of the feedstock [4]. Before being processed in the refinery, the PYGAS stream must be stabilized to eliminate unstable components, particularly diolefins and styrene, otherwise these compounds would react downstream over the catalysts, forming polymeric deposits and causing deactivation and increase of the pressure drop [5]. The customary industrial solution for stabilization is hydrogenation. This however must be highly selective because the integrity of the aromatic rings in benzenoid compounds and of the double bond in monoolefins should be preserved either for provision of octane number during gasoline blending or for supplying feedstocks for polyolefins units. Generally speaking the compound most refractory to hydrogenation is styrene. For this reason it is usually adopted as a model compound in lab scale tests of selective hydrogenation [6, 7].

In previous works we have reported that monometallic Pd catalysts prepared from chlorinated precursors are more active, sulfur and oxygen resistant than similar Pd catalysts prepared from nitrogenated salts or other noble metal catalysts (Pt, Ru and Rh) [6, 8]. We have also reported that when Pd is supported over composite organic-inorganic supports, the resulting catalysts prove to be highly active for the selective hydrogenation of styrene [9]. These catalysts were also found to be more mechanically resistant than other commercial supports thus being attractive for being used in long packed bed columns of continuous processes [10]. Finally they have been also found to permit an easy preparation of supported metal egg-shell catalysts with very thin surface metal layers [10, 11]. Despite their practical usefulness there are scarce reports on the use of these composite supports [12]. Particularly there are practically no kinetic studies for these catalysts on the selective hydrogenation of vinylic bonds, such as those present in styrene.

The objective of this work is to study the kinetics of the selective hydrogenation of styrene to ethylbenzene, using a catalyst of Pd supported over an organic-inorganic composite support. The focus is put on obtaining an insight into the working reaction mechanism and on obtaining global kinetic rate equations. The latter should prove to be useful for optimization of reaction conditions, simulation of reactors and scale-up of packed units with these composite catalysts.

Experimental

Catalyst preparation

The composite support (BTAl) was prepared following a technique developed by our group [9, 10]. The method basically comprises the copolymerization of two monomers (1:1 molar ratio). BTAl is an acronym used for the composite support made from three different components: Bisphenol A glycerolatedimethacrylate (BGMA) and Triethylene glycol dimethacrylate (TEG) in a mixture with Alumina (45 wt%, 200 meshes) as inorganic filler. The final material was extruded into cylindrical pellets of 3 mm length and 1 mm diameter.

Palladium was deposited over the support by means of incipient wetness impregnation. BTAl pellets were impregnated with an aqueous acidic solution of $PdCl_2$ (Fluka, Cat Nº: 76050, purity >99.98%) at a pH value of 1. The volume and concentration of the impregnating solution were adjusted in order to obtain ca. 0.3 wt% of Pd in the final catalyst. The pellets were then dried at 393 K for 24 h in an oven, milled to a fine powder, particle size being lower than 120 meshes, and then stored in a desiccator for later use. Before the catalytic tests the catalysts were reduced in situ in flowing hydrogen (100 mL min^{-1} g_{cat}^{-1}) at 483 K for 1 h.

Catalyst characterization

The specific surface area (S_{BET}) was measured by means of nitrogen adsorption at 77 K using a Quantachrome NOVA-1000 apparatus. The samples were first degassed overnight at 523 K in a vacuum (<10^{-9} bar).

The palladium content of the catalysts was obtained by digesting the sample and then analysing the liquors in a Perkin Elmer Optima 2100 DV ICP equipment.

X-ray diffractograms were obtained in a Shimadzu XD-1 equipment, using CuKα radiation (λ=1.5405 Å) filtered with Ni and scanning the 20-70º 2Θ range.

Electron probe micro analysis (EPMA) measurements were performed in a JEOL JSM-35C instrument equipped with an energy dispersion system (EDAX). Samples to be analysed were previously coated with carbon in a vacuum deposition. The scanning speed was 0.02 mm min^{-1} and the acceleration voltage of the electron beam was 20 kV.

The superficial electronic state of Pd metal and chlorine and their atomic ratios were obtained by X-ray Photoelectron Spectroscopy (XPS) in a VG-Microtech Multilab equipment, using the Pd $3d_{5/2}$ and Cl $2p_{3/2}$ peaks. Radiation was MgKα (1253.6 eV) and a pass energy of 50 eV was used. The system pressure was kept at 5 x 10^{-12} bar. Samples were prereduced in situ 1 h at 483 K .To correct possible deviations caused by electronic charge on the samples, the Al 2p line was taken as an internal standard at 74.4 eV. The areas under the peaks were estimated by calculating the integral of each peak after subtracting the Shirley background and fitting the experimental peak to a combination of Lorentzian and Gaussian lines of 30–70% proportions [13].

Catalytic tests

The hydrogenation reaction of styrene to ethylbenzene was performed in batch mode using a PTFE coated, stainless steel, stirred tank reactor. In each test the reactor was charged with 200 mL of a solution of styrene in *n*-octane. Styrene was supplied by Aldrich (Cat. N° S497-2, purity > 99%) and *n*-octane by Merck (purity > 99%). *n*-Decane (Fluka, Cat. N° 30550, purity > 98%) was used as an internal standard. The catalyst mass used was 100 mg and the particle size was lower than 120 meshes. Reaction conditions were varied in order to assess their influence on the reaction rate: hydrogen pressure=10, 20 and 30 bar, initial styrene concentration=0.260, 0.434 and 0.607 M, temperature=353, 373 and 393 K. These conditions were chosen in order to mimic industrial conditions in selective hydrogenation units. Before the catalytic tests the catalysts were reduced in situ in flowing hydrogen (100 mL min^{-1} $gcat^{-1}$) at 483 K for 1 h.

Samples were taken at different values of reaction time and analyzed by gas chromatography in a Shimadzu 2014 gas chromatograph equipped with a FID detector and a 30 m J&W InnoWax 19091N-213 (cross-linked polyethylene glycol phase) capillary column.

Mathematical calculations

The treatment of the kinetic data was done using ad-hoc programs and software tools contained in the MatLab for Windows software package (R2013b version). The basic calculation tasks comprised: (i) the integration of the ordinary differential

equations describing the evolution of the concentration of the different reacting species in the system; (ii) the optimization of the parameters of the different models tried. On the one hand, (i) was performed by using the module ODE45 of MatLab, a medium order solver for non-stiff differential equations that is based on an explicit Runge-Kutta (4, 5) formula, the Dormand-Prince pair [14]. This is a one-step solver that needs only the solution at the immediately preceding time point. On the other hand (ii) was implemented by minimizing the sum of the squares of the deviations between the real (experimental) and predicted (model) concentration values. Only styrene concentration values were used to build the sum of squares because adding ethylbenzene or other concentration values did not yield a better error measure.

Minimization of the sum of squares was performed using both the MatLab routines FMINCON and FMINSEARCH. It was found that FMINCON could better find regions of optimality starting from an arbitrary seed point while FMINSEARCH was better for refining the solution. FMINCON finds the minimum of a constrained nonlinear multivariable function. Constraints were built from the condition of positivity of the model parameters. FMINCON used the interior-point algorithm [15] with no user-supplied Hessian. FMINCON is a gradient-based method designed to work on problems where the objective and constraint functions are both continuous and have continuous first derivatives. FMINSEARCH is an unconstrained nonlinear optimization module that uses the Simplex search method of Lagarias et al [16]. This is a direct search method that does not use numerical or analytical gradients. The handling of the constraints of positivity of the parameters was handled in this case by adding a penalty term to the objective function anytime the constraint was violated.

The set of ordinary differential equations is described in equations (1) to (6), with A=styrene, B=ethylbenzene, H_2=hydrogen. These equations describe the concentration of the species in a closed, discontinuous, perfectly mixed reactor. Given the high excess of hydrogen of all tests the variation of the hydrogen concentration was considered to be negligible (eq. (3)).The partial pressure of hydrogen was calculated by subtracting the equilibrium pressure of solvent from the total pressure. The vapor pressure of n-octane was calculated with Antoine's formula and parameters as tabulated in NIST database and based on reported data of Carruth and Kobayashi [17]. Vapor pressure values at 353, 373 and 393 K were 0.24, 0.52 and 1.01 bar.

For all the experimental conditions, global selectivities to the desired product in excess of 98% were obtained, so the equations representing other lateral reactions, such cracking and oligomerization were not considered. The solvent is supposed not to participate in any reaction.

$$\frac{dC_A}{dt} = -r \tag{1}$$

$$\frac{dC_B}{dt} = r \tag{2}$$

$$\frac{dP_{H2}}{dt} \approx 0 \tag{3}$$

$$C_A = C_A^0 \quad for \quad t = 0 \tag{4}$$

$$C_B = 0 \quad for \quad t = 0 \tag{5}$$

$$P_{H2} = P_{total} - P^o_{solvent} \tag{6}$$

The formula for the sum of squares, χ^2, the objective function to be minimized is eq. (7). In this equation *i* is the number of the experiment in the data set and *j* is the point number of the run. $C_{i,j}$ is the experimental data point and $C_{i,j}^{CALC}$ is the corresponding point as calculated by the integration of the used model

$$\chi^2 = \sum_j^n \left(C_{i,j} - C_{i,j}^{CALC}\right)^2 \tag{7}$$

r denotes the reaction rate, which generally has two terms, r_{dir}, the rate of the direct reaction, and r_{inv}, the rate of the inverse reaction. The inverse reaction rate was considered negligible on attention to the value of the thermodynamic equilibrium constant at the reaction conditions. This was calculated from the data reported by Abo-Ghanderet al. [18] for the dehydrogenation of ethylbenzene to styrene (see eqs. (8) and (9), *T* in K, ΔF in Cal mol^{-1} K^{-1}). The values at 353 and 373 K for the hydrogenation of styrene were calculated as K_{eq}=3.38x10^{11} and K_{eq}=3.57x10^{10}, respectively. With these K_{eq} values the reaction of styrene hydrogenation is practically irreversible.

$$K_{eq} = e^{(-\Delta F / RT)} \quad (8)$$

$$\Delta F = (122725.16 - 126.27\,T - 0.002194\,T^2)\,0.238 \quad (9)$$

r_{dir} has a Langmuir-Hinshelwood form, given the convolution of adsorption and reaction phenomena. See eq. (11) as an example. In this equation k is a kinetic constant and K_A and K_{H2} are adsorption constants. Kinetic and adsorption equilibrium constants can be further described as functions of the temperature, activation energy and heat of adsorption (eqs. (12) and (13)).

$$r = r_{dir} - r_{inv} \approx r_{dir} \quad (10)$$

$$r_{dir} = \frac{k'\,C_A\,C_{H2}}{1 + K_A C_A + K'_{H2}\,C_{H2}} \quad (11)$$

$$k' = A\,e^{-Ea/RT} \quad (12)$$

$$K_{ads} = B\,e^{-\Delta H / RT} \quad (13)$$

Reactions occur on the catalyst surface and the reactants are styrene and dissolved hydrogen. Hydrogen dissolution is dictated by Henry's law (eq. (14)). In this equation H is Henry's constant that is practically a linear function of temperature in the working range. In the case of isothermal data H can be lumped with the adsorption and kinetic constants to give new global constants. For non-isothermal data sets the lumping can still be done if the variation in the value of H is not too high. Otherwise a linear equation to reflect the temperature dependence of H must be added (eq. (15)). According to reported experimental data [19] the value of H is about 210 bar L mol^{-1} with a variation of 3% in the 353-373 K range. This variation is considered negligible and therefore the rate equations will be directly formulated in terms of P_{H2} as in eq. (11) for the sake of simplicity.

$$C_{H2} = \frac{P_{H2}}{H} \quad (14)$$

$$H = D + E\,T \quad (15)$$

Taking H as approximately constant, equation (11) can be rewritten in terms of hydrocarbon reactant concentrations and hydrogen pressure (eq. (16)) with the help of eqs. (17) and (18).

$$r_{dir} = \frac{k\,C_A\,P_{H2}}{1 + K_A C_A + K_{H2} P_{H2}} \quad (16)$$

$$k = \frac{k'}{H} \quad (17)$$

$$K_{H2} = \frac{K'_{H2}}{H} \quad (18)$$

Results and discussion

Catalyst characterization

The catalysts used for this work were the same as those used in our previous contribution [11] and share the same characterization results. For this reason only the most relevant data necessary for interpreting the kinetic results will be repeated here. For a more detailed description of the characterization of these composite catalysts the reader is referred to our recent reports [11, 20].

The BET surface area was 1.1 m^2g^{-1} for the 0.3PdBTAl composite catalyst. This is a low value of surface area if we compare with the value for the γ-alumina component (224 m^2g^{-1}). Given the relatively high mass percentage of alumina present (45%) it can be inferred that the polymer coats the alumina particles blocking most pore mouths.

The Pd content of the prepared catalyst was 0.26 wt% as determined by ICP-OES.

The X-ray diffractograms of the 0.3PdBTAl catalyst, the BTAl support and the alumina component are presented in Fig. 1. The diffractograms have been mathematically smoothed for a better readability. As it can be seen both diffractograms are identical, with peaks at 37.7, 46.0 and 67.0° due to the gamma phase of alumina. This indicates that the polymerization of the organic component of the composite produced only an amorphous phase. The diffractogram of the reduced 0.3PdBTAl catalysts displayed an additional shoulder at 2θ=39.9º that was attributed to the reflection of the Pd (111) plane. Other secondary peaks of the Pd phase could not be detected.

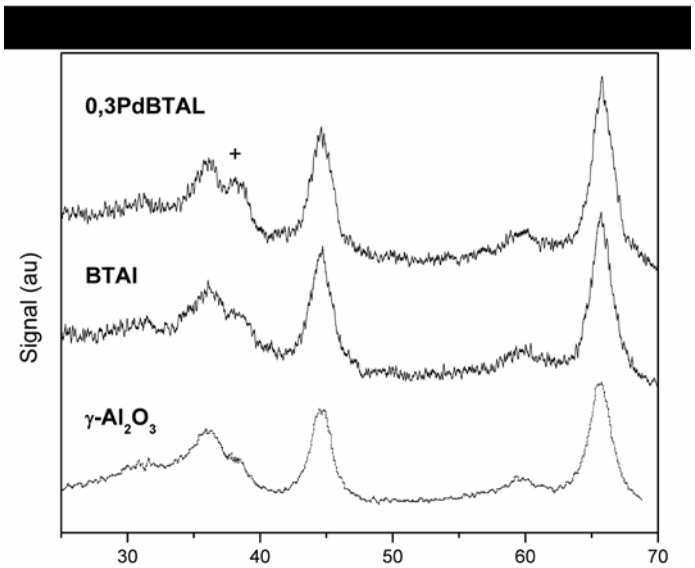

Fig. 1 X-ray diffractograms of the supports and the Pd catalyst [20]. (+) Pd.

Characterization by EPMA confirmed the egg-shell pattern of the 0.3Pd/BTAl catalyst (see Figure 2). The average thickness of the egg-shell zone as determined by EPMA was 22 μm. The results point to a pattern of Pd distribution made of two contributions: a homogeneous core level, of 1.01% the total Pd charge at $0 \leq R'/R \leq 0.93$ and a surface layer contribution of 98.99% at $0.93 \leq R'/R \leq 1$ (R′: radial coordinate, R: particle radius).

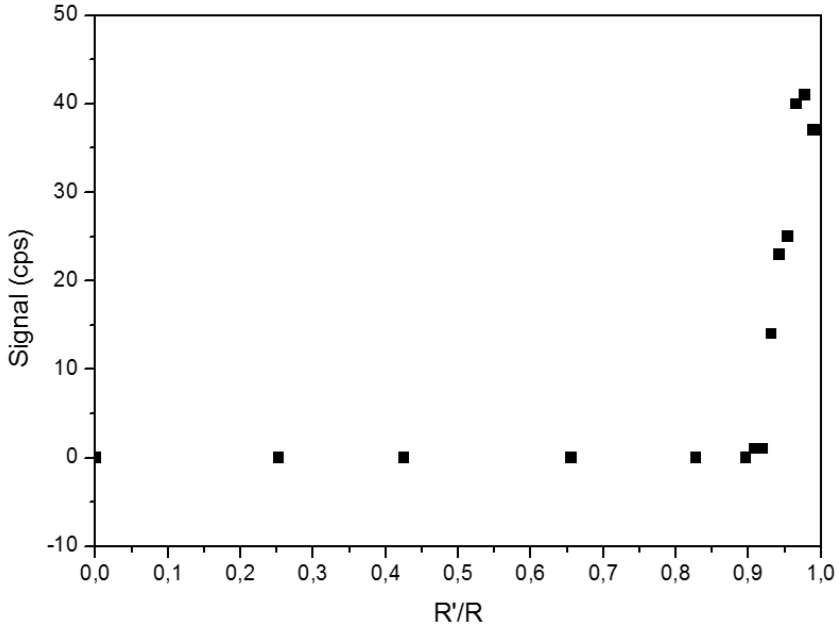

Fig. 2 Pd penetration profile in the 0.3PdBTAl catalyst as determined by EPMA [11].

The XPS analysis of the Pd $3d_{5/2}$ peak showed two components, one at 335.6 eV (75.6%) attributed to $Pd^{\delta+}$ (with $\delta \cong 0$) and another at 336.6 eV (24.4%) attributed to Pd^{n+} (with $n \cong 2$). If we recall the XRD results, the $Pd^{\delta+}$ should be metallic, though slightly electrodeficient. Pd^{n+} is electrodeficient most likely because of the presence of refractory oxychloride $Pd_xO_yCl_z$ species or non-reduced Pd species stabilized by adjacent Cl atoms [21-24].

Assessment of kinetic regime

In all the catalytic tests practically the only product detected by gas chromatography was ethylbenzene. The final selectivity was higher than 99%, as calculated by the internal standard method. A first stage of preliminary tests was performed in order to check the absence of mass transfer limitations. In these tests the reaction temperature, pressure, catalyst mass, styrene initial mass and solvent mass were kept constant and the stirring rate was varied in the 500-1400 rpm range and it was found that at rates higher than 800 rpm the conversion of styrene remained constant. A stirring rate of 1200 rpm was then chosen for all the reaction tests to ensure that the reaction was not limited by a gas-to-liquid mass transfer resistance related to insufficient stirring.

To further evaluate the magnitude of the external gas-to-liquid mass transfer resistance the reaction rate was evaluated at different values of catalyst concentration and the inverse of the initial reaction rate was plotted as a function of the inverse of the catalyst concentration. According to the theory of slurry reactors the interplay of the different resistances would be described by equations (19-21) for the reaction rate of a system with pseudo first order dependency with respect to the concentrations of dissolved hydrogen [25]. In equation (19) k_L is the liquid film transfer coefficient, k_c is the liquid-solid film transfer coefficient, a_c is the external catalyst surface, a_g is the gas-liquid interface area, m_c is the catalyst concentration, k is the pseudo first order global kinetic constant and ξ is the intraparticle reaction efficiency.

$$r = \frac{C_{H2(liq)}}{\frac{1}{k_L\, a_g} + \frac{1}{m_c}\left(\frac{1}{k_c\, a_c} + \frac{1}{k\, \xi}\right)} \qquad (19)$$

$$r = \frac{\left(\frac{P_{H2(gas)}}{H}\right)}{R_{G-L} + R_{S-L} + R_{D-R}}, \quad C_{H2(liq)} = \frac{P_{H2(gas)}}{H} \tag{20}$$

$$\left(\frac{C_{H2(liq)}}{r}\right) = R_{G-L} + \frac{1}{m_c}\left(\frac{1}{k_c\, a_c} + \frac{1}{k\, \xi}\right) \tag{21}$$

As it can be seen from equations (19-21) the intercept of the line of ($C_{H2(liq)}/r$) as a function of $1/m_c$, should be equal to R_{G-L}, the gas-liquid mass transfer resistance. A plot of this kind was made using initial reaction rate data. The linear regression of the data in the plot of Fig. 3 (r^2=0.918) yields a slope of 0.03672 and an intercept of (-0.03713). The intercept of the line is negative and close to zero, which means the gas-liquid resistance is practically zero.

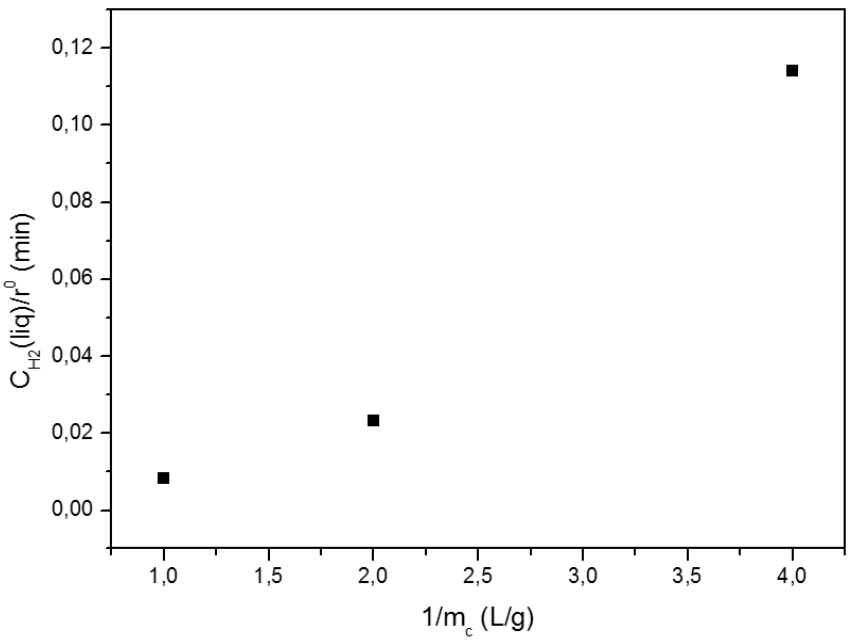

Fig. 3 Assessment of the gas-liquid mass transfer resistance. Plot of the ratio (hydrogen concentration / initial reaction rate) as a function of the inverse of the catalyst concentration

Finally, the solid-liquid resistance was considered to be also negligible due to the reduced particle size used, lower than 120 US mesh (< 125 μ). A verification of this was made by calculating the Damköhler number (*Da* < 0.001) with the maximum value of the reaction rate (about 3 mol L^{-1} h^{-1}) and an estimation of the k_c (film mass transfer coefficient) value in the stirred reactor at the reaction conditions (particle diameter d_p=25 μ, $D_{H2,liq}$=0.0002 cm^2 s^{-1},$C_{H2,liq}$=0.074 mol L^{-1}, m_c=0.1 g, 20 bar total pressure, 353 K reaction temperature) under the most unfavourable solid-liquid conditions (no slip velocity, *Sh*=2). *Da* and *Sh* are the Damköhler and Sherwood numbers, d_p, D_{H2}, C_{H2} and m_c are the catalyst particle diameter, the molecular diffusivity of hydrogen (as calculated with the Wilke-Chang equation) in the solvent, the concentration of hydrogen in the solvent and the catalyst mass, respectively.

Kinetic data organization and preliminary analysis

The experimental points were classified into two sets, isothermal and complementary. A full description is included in Table 1. The isothermal data set comprised 5 runs performed at 373 K that were used to make a first selection of the most promising models that did not involve the regression of activation energies or heats of adsorption. The full data set comprised both the isothermal and complementary runs at 353 and 393 K and was used to make a final choice of the models giving a better fit of the experimental data and a regression of the energy parameters.

$$r = k\, C_A^m P_{H2}^n \tag{22}$$

A preliminary analysis of the data was done by analysing subsets with most variables constant and with only varying hydrogen pressure (runs 2, 3 and 4) and varying styrene initial concentration (runs 1, 3 and 5). Fitting of a potential law kinetic rate model as depicted in equation (22) with initial reaction rate values (r^0, extrapolation to t=0) yields n=0.12 and m=-0.36. Considering eq. (22) as an approximation of a general Langmuir-Hinshelwood rate expression such as (11), the value of m might indicate that there exists a strong adsorption of styrene on the surface active sites of the catalyst. The value of n can be due to a low order in the driving force term of the rate equation (numerator) or a relatively important adsorption of hydrogen at the working conditions.

Table 1 Description of the experimental data set

Data set name		Run	Temperature, K	Pressure, bar	Initial styrene concentration, mol L^{-1}	Number of points	Reaction time, min
Full	Isothermal	1	373	20	0,607	18	420
		2	373	10	0.434	16	300
		3	373	20	0.434	17	330
		4	373	30	0.434	16	300
		5	373	20	0.260	11	150
	Complementary	6	353	20	0,434	18	360
		7	393	20	0.434	13	210

Using runs 3, 6 and 7 to obtain r^0 values at 353, 373 and 393 K and fitting the data of $ln(r^0)$ vs $(1/T)$ with a linear relation permits obtaining an approximate value of the activation energy (slope of the plot), 9.9 kCal mol^{-1}. This can be compared with the values obtained by other authors for the liquid phase hydrogenation of styrene (see Table 2). It can be seen that the present value for the apparent activation energy is similar to that of other systems of palladium supported over activated carbon. This might be related to the chemical similarity between the amorphous polymer and amorphous activated carbon.

Table 2 Comparison of the apparent activation energy (E_a^{app}) for styrene hydrogenation reported in the literature

System	Reference	wt % Pd	Solvent	E_a^{app}, kCal mol^{-1}
0.3PdBTAl	-	0.3	Octane	9.9
Pd/SiO_2	[26]	0.09	Heptane	5.5
Pd/Al_2O_3	[27]	0.3	Toluene	3.6
Pd/C	[28]	3	Methanol	9.5
Pt/C	[28]	5	Methanol	11.4
Pd/Al_2O_3	[29]	0.3	Heptane	6.2
Pd/C	[30]	1	Dodecane	9.8
Pd/Al_2O_3	[31]	0.4	Toluene	6.4

Kinetic modeling

Different models were built using the Hougen-Watson formalism. With this methodology a chain of elementary steps must be written down to completely describe the working mechanism. Then one elementary step must be chosen as the slowest and that will be the rate-limiting step. All other elementary steps are considered in equilibrium. These equilibrium and rate equations do not yield a determinate system and additional equations must be obtained. This can be done by using the balance of adsorption sites. These balances yield Langmuir like equations that in the end generate the so-called Langmuir-Hinshelwood-Hougen-Watson kinetic rate models.

The formulation of the elementary steps of the mechanism needs a set of hypotheses related to the working surface phenomena. In the case of the studied system the following assumptions were made:

(i) Only one reaction mechanism is acting over the whole range of conditions used.

(ii) The adsorption of hydrogen and the adsorption of styrene are competitive, i.e. they occur on the same type of site. This hypotheses can be found in other reports on styrene hydrogenation such as that of Corvaisier et al [26]. Ali [32] studied the hydrogenation of pyrolysis gasoline and determined zero order kinetics in the case of styrene hydrogenation due to the competitive strong adsorption of styrene. Chou and Vannice [33] found that benzene and hydrogen adsorption became competitive at temperatures higher than 300 K. According to the XPS data the adsorption site for both hydrogen and styrene adsorption would be a Pd electrodeficient metal site.

(iii) The chemisorption of hydrogen over Pd is dissociative. Dissociative adsorption of hydrogen on Group VIII metals is well established, and this form is frequently invoked when modelling hydrogenation reactions [34].

(iv) During the reaction the concentration of hydrogen, both in the gas and liquid phases, is considered to be constant. This means that the liquid phase is not depleted of dissolved hydrogen and the hydrogen dissolution equilibrium is fast enough. This is assumed because a high and efficient stirring rate is used, the reactant is highly diluted in the solvent and a constant high hydrogen pressure is used.

(v) The hydrogenation of adsorbed styrene occurs by insertion of one hydrogen atom at a time like in the classic Horiuti-Polanyi mechanism for hydrogenation [35, 36].

(vi) The adsorption of ethylbenzene is a priori non-negligible.

(vii) The adsorption of the solvent on the catalyst surface active sites is considered to be negligible.

(viii) The hydrogenation reaction is irreversible. As mentioned before and according to the data reported by Abo-Ghander et al. [18] (eqs. (8) and (9)), the equilibrium constant for hydrogenation of the double bond is in the order of 10^{10}-10^{11} in the temperature range of this work.

(ix) The mechanism proceeds either with a fraction of the active sites covered (non-saturated surface) or with all active sites covered by adsorbates (saturated surface).

(x) The occurrence of side reactions like cracking, oligomerization, aromatic ring aromatization is disregarded on the basis of the measured high selectivity of the catalyst.

Taking into account the previous hypotheses, the elementary steps of Table 3 can be written down.

Table 3 Elementary steps to be considered in the global mechanism

Elementary steps description	Reactions	Equilibrium equation
Hydrogen dissociative chemisorption	$H_2 + 2S \longleftrightarrow 2HS$	$K_{H2} = \frac{C_{HS}^2}{P_{H2} C_S^2}$
Styrene adsorption	$A + S \longleftrightarrow AS$	$K_A = \frac{C_{AS}}{C_A C_S}$
Surface two-step hydrogenation reaction (Horiuti-Polanyi)	$HS + AS \longleftrightarrow AHS + S$	$K_{S1} = \frac{C_{AHS} C_S}{C_{HS} C_{AS}}$
	$HS + AHS \longleftrightarrow BS + S$	$K_{S2} = \frac{C_{BS} C_S}{C_{AHS} C_{HS}}$
Ethylbenzene desorption	$BS \longleftrightarrow B + S$	$\frac{1}{K_B} = \frac{C_B C_S}{C_{BS}}$

The different choice of rate-limiting steps and considering a partially saturated or fully saturated surface leads to different LHHW models that are depicted in Table 4. In this table k is the true kinetic constant of the rate-limiting step, K_{H2}, K_A and K_B are the thermodynamic constants for the adsorption of hydrogen, styrene and ethylbenzene, respectively. K_{S1} and K_{S2} are the equilibrium constants of the two steps of the Horiuti-Polanyi surface reactions. The condition of non-saturated surface occurs when the values of the adsorption constants are sufficiently small to allow the existence of a non-negligible fraction of free adsorption sites.

Table 4 Different LHHW models studied and their underlying assumptions. Descriptive reaction rate formula r (with all kinetic and thermodynamic parameters) and simplified reaction rate formula r* (with minimum number of independent adjustable parameters)

	Model assumptions	Reaction rate formula	Simplified reaction rate formula
1	H_2 adsorption is rate-limiting. Non-saturated surface.	$r = \frac{k_{H2} C_{ST}^2 P_{H2}}{\left(1 + K_A C_A + K_B C_B\right)^2}$	$r^* = \frac{P_{H2}}{\left(P_1 + P_2 C_A + P_3 C_B\right)^2}$
2	Styrene adsorption is rate-limiting. Non-saturated surface.	$r = \frac{k_A C_{ST} C_A}{\left(1 + \sqrt{K_{H2} P_{H2}} + K_B C_B\right)}$	$r^* = \frac{C_A}{\left(P_1 + P_2 \cdot \sqrt{P_{H2}} + P_3 C_B\right)}$
3	H_2 adsorption is rate-limiting. Saturated surface.	$r = \frac{k_{H2} C_{ST}^2 P_{H2}}{\left(K_A C_A + K_B C_B\right)^2}$	$r^* = \frac{P_{H2}}{\left(P_1 C_A + P_2 C_B\right)^2}$
4	Styrene adsorption is rate- limiting. Saturated surface.	$r = \frac{k_A C_{ST} C_A}{(\sqrt{K_{H2} P_{H2}} + K_B C_B)}$	$r^* = \frac{C_A}{\left(P_1 \sqrt{P_{H2}} + P_2 C_B\right)}$
5	Formation of half-hydrogenation intermediate is rate-limiting. Non-saturated surface	$r = \frac{k_{S1} C_{ST}{}^2 K_A \sqrt{K_{H2} P_{H2}} C_A}{\left(1 + \sqrt{K_{H2} P_{H2}} + K_A C_A + K_B C_B\right)^2}$	$r^* = \frac{\sqrt{P_{H2}} C_A}{\left(P_1 + P_2 \sqrt{P_{H2}} + P_3 C_A + P_4 C_B\right)^2}$
6	Insertion of second hydrogen atom is rate-limiting. Non-saturated surface.	$r = \frac{k_{S2} C_{ST}{}^2 K_A K_{H2} K_{AH} P_{H2} C_A}{\left(1 + \sqrt{K_{H2} P_{H2}} + K_{S1} K_A C_A \sqrt{K_{H2} P_{H2}} + K_A C_A + K_B C_B\right)^2}$	$r^* = \frac{P_{H2} C_A}{\left(P_1 + P_2 \sqrt{P_{H2}} + P_5 P_2 P_3 \sqrt{P_{H2}} C_A + P_3 C_A + P_4 C_B\right)^2}$
7	Formation of half-hydrogenation intermediate is rate-limiting. Saturated surface.	$r = \frac{k_{S1} C_{ST}{}^2 K_A \sqrt{K_{H2} P_{H2}} C_A}{\left(\sqrt{K_{H2} P_{H2}} + K_A C_A + K_B C_B\right)^2}$	$r^* = \frac{\sqrt{P_{H2}} C_A}{\left(P_1 \sqrt{P_{H2}} + P_2 C_A + P_3 C_B\right)^2}$
8	Insertion of second hydrogen atom is rate-limiting. Saturated surface.	$r = \frac{k_{S2} C_{ST}{}^2 K_A K_{H2} K_{AH} P_{H2} C_A}{\left(\sqrt{K_{H2} P_{H2}} + K_{S1} K_A C_A \sqrt{K_{H2} P_{H2}} + K_A C_A + K_B C_B\right)^2}$	$r^* = \frac{P_{H2} C_A}{\left(P_1 \sqrt{P_{H2}} + P_4 P_2 P_3 \sqrt{P_{H2}} C_A + P_2 C_A + P_3 C_B\right)^2}$

As an example, the constitutive equations of Model 5 that considers the formation of half-hydrogenation intermediate as the rate-limiting step and a non-saturated surface, are written below:

$$K_{H2} = \frac{C_{HS}^2}{C_S^2 \, P_{H2}} \qquad \text{(equilibrium) (23)}$$

$$K_A = \frac{C_{AS}}{C_S\, C_A} \quad \text{(equilibrium) (24)}$$

$$r = k_S C_{AS} C_{HS} \quad \text{(rate limiting step) (25)}$$

$$\frac{1}{K_B} = \frac{C_B\, C_S}{C_{BS}} \quad \text{(equilibrium) (26)}$$

$$C_{ST} = C_S + C_{HS} + C_{AS} + C_{BS};\ C_{HAS} \approx 0 \quad \text{(balance of adsorption sites)(27)}$$

In equation (27) the concentration of the intermediate half hydrogenated species is considered to be negligible. This is because the half hydrogenated species is not stable and should rapidly accept another hydrogen while it is still in the adsorbed state [20].

Isothermal data fitting. The fitting of the isothermal data set using the MatLab optimizers yielded the results described in Table 5. A limit of χ^2=0.05 was used to keep or reject the models.

Table 5 First screening of the models using the isothermal data set

Model	Rate controlling step	Surface Saturation	X^2	Result
1	Hydrogen adsorption	No	0.2243	Rejected
2	Styrene adsorption	No	0.0669	Rejected
3	Hydrogen adsorption	Yes	2.4967	Rejected
4	Styrene adsorption	Yes	0.0685	Rejected
5	Insertion of 1st hydrogen	No	0.0157	Kept
6	Insertion of 2nd hydrogen	No	0.0246	Kept
7	Insertion of 1st hydrogen	Yes	0.0157	Kept
8	Insertion of 2nd hydrogen	Yes	0.0246	Kept

Models in Table 4 which did not have hydrogen adsorption terms (1 and 3) produced the poorest fit, and models that adjusted the data better were those based on surface reaction as rate limiting step (5 to 8). In these optimization runs it was found that models supposing a saturated surface (negligible concentration of free active sites, models 7 and 8) adjusted the data set with the same error that models with an extra parameter, like 5 and 6, due to consider non saturated surface.

Based on the error level (χ^2=0.05) the original set of models was reduced to only four: Models 5, 6, 7 and 8.

Full data fitting. These four models were then tested with the full data set (isothermal and non-isothermal) to obtain their error and the value of the model parameters. A full model with temperature dependent parameters is written below as an example for Model 5 (eqs. (28) to (36)). Once the thermal parameters P_i are determined from regression of the full data set, most of the parameters in equation (28) can be calculated. Others, like the pre-exponential factors, cannot be calculated without information on the value of C_{ST}, the total concentration of active sites.

For some models with *N* thermochemical parameters the regression procedure yielded only (*N-1*) significant parameters and one of them had to be estimated from literature references. This was the case for the models that supposed a saturated surface: 7 and 8. In these models the elimination of the term associated to the free surface sites reduces the number of fitting parameters by one. For these cases the heat of dissociative chemisorption of H_2 was considered to be known and the value reported by Conrad et al. [37] was adopted (-26 kCal mol^{-1}).

In Table 6 are reported the values of the fitting error (χ^2) and the model selection criterion (MSC) for the full data set and the corresponding regressed parameters: E_a, ΔH_A, ΔH_B, ΔH_{H2} and ΔH_{AH}. ΔH_{AH} is the heat of the equilibrium reaction for the first semi-hydrogenation in models 6 and 8. The model adequacy and the discrimination between models were determined using the model selection criterion (MSC), according to the following equation:

$$MSC = \ln\left[\frac{\sum_{i=1}^{n}\left(C_i - C_{AV}\right)^2}{\sum_{i=1}^{n}\left(C_i - C_i^{CALC}\right)^2}\right] - \left(\frac{2.p}{n}\right) \quad (37)$$

where n is the number of experimental data, p is the amount of parameters fitted, C_{AV} is the average relative concentration and C_i^{CALC} and C_i are the predicted and experimental values, respectively. When various different models are compared the most significant one is that with the highest MSC value.

Comparing the values of MSC for the full data set of Models 5 to 8 in Table 6, we can see that the values are higher for Models 5 and 7 that also have the lowest values of χ^2. According to the results of Table 6 the mechanism that better fits the data is that one supposing the surface reaction as limiting step and specifically the insertion of the first hydrogen in the molecule. This agrees with a classical Horiuti-Polanyi mechanism with concurrent competitive adsorption of hydrogen, styrene and ethylbenzene. Of the two variants (Models 5 and 7), Model 7 that supposes a negligible fraction of free adsorption sites, yields a similar error with fewer adjusting parameters. Moreover in the case of Model 5, the presence of the extra parameter enabled obtaining many solutions with similar error but widely differing values of the adjusted parameters, indicating that the solution was not a robust one. Therefore the best fitting model is Model 7.

Table 6 Values of the fitting error (χ^2) for the full data set (isothermal and non-isothermal) and the corresponding regressed parameters of the best model

Model	$\chi 2$	*MSC*	E_a kCalmol^{-1}	ΔH_A kCal mol^{-1}	ΔH_B kCalmol^{-1}	ΔH_{H2} kCalmol^{-1}	ΔH_{AH} kCalmol^{-1}
5	0.0216	4.42	16.8	-11.5	-11.6	-23.1	-----
6	0.0316	4.04	13.0	-3.90	-6.63	-20.4	10.5
7	0.0216	4.42	18.2	-12.9	-13.0	-26.0	-----
8	0.0299	4.09	18.0	-6.19	-12.2	-26.0	7.40

Table 7 contains values of the Arrhenius and van't Hoff parameters of Model 7 as obtained by regression of the full set of kinetic data. It can be seen that within the experimental error, the heats of adsorption of ethylbenzene and styrene are almost equal, about -13 kCal mol^{-1}. The sign of the heat of adsorption agrees with the general trend of entropy decreasing during adsorption. A direct comparison of the found values of the heats of adsorption of ethylbenzene and styrene with reported values is not possible due to the availability of only scarce information for the Pd-styrene system. A comparison with other supported catalysts should be considered cautiously. Zhou et al. [38] reported a heat of adsorption of -3.2 kCal mol^{-1} for styrene on Pd/Al_2O_3. Ranke and Joseph [39] reported values of the heat of adsorption of ethylbenzene and styrene over FeO(111) of -13.9 kCal mol^{-1} and -13.5 kCal mol^{-1}, respectively. For ethylbenzene on Ni/Al_2O_3 Smeds et al. [40] reported a heat of adsorption of -30 ±18 kCal mol^{-1}. Chaudari et al. [41] have found that the adsorption of ethylbenzene and styrene are similar but much smaller than the adsorption of phenyl acetylene, the latter being highly detrimental to the hydrogenation reaction rate.

Table 7 Energy parameters and fully detailed expressions of the best fitting model

$$r = \frac{k_{S1} C_{ST}^{\ 2} K_A \sqrt{K_{H2} P_{H2}}\, C_A}{\left(\sqrt{K_{H2} P_{H2}} + K_A C_A + K_B C_B\right)^2}$$

$$k_{S1} = a_{S1} e^{-E_a / RT}$$

$$K_A = a_A e^{-\Delta H_A / RT}$$

$$K_B = a_B e^{-\Delta H_B / RT}$$

$$K_{H2} = a_{H2} e^{-\Delta H_{H2} / RT}$$

$$r = \frac{a_{S1} e^{-E_a / RT} C_{ST}^{\ 2} a_A e^{-\Delta H_A / RT} \sqrt{a_{H2}}\, e^{-\Delta H_{H2} / 2RT} \sqrt{P_{H2}}\, C_A}{\left(\sqrt{a_{H2}}\, e^{-\Delta H_{H2} / 2RT} \sqrt{P_{H2}} + a_A e^{-\Delta H_A / RT} C_A + a_B e^{-\Delta H_B / RT} C_B\right)^2}$$

$$E_1 = E_a + \frac{\Delta H_{H2}}{2} + \Delta H_A$$

Property	Value and units
E_a	18.2 kCal mol^{-1}
ΔH_A	-12.9 kCal mol^{-1}
ΔH_B	-13.0 kCal mol^{-1}
ΔH_{H2} [34]	-26.0 kCal mol^{-1}

The weak adsorption of hydrogen on palladium as compared to styrene and ethylbenzene could have been enhanced by the electrodeficient state of the metal particles. Singh and Vannice [42] noted that hydrogen adsorption is weak over $Pd^{\delta+}$ due to the depletion of *d* electrons by adjacent electronegative species. The electrodeficiency of Pd would also reduce the equilibrium concentration of available surface atomic hydrogen and would slow down the hydrogenation steps, probably favoring in this way the existence of the half hydrogenated intermediate [20]. Electrodeficiency would also enhance the adsorption of styrene and ethylbenzene. In this sense it has been reported [43] that the higher the electrodeficiency of the metal, the stronger the adsorption of aromatic compounds, the effect being related to an increase in the unoccupied states in the metal *d* band. In an example of the opposite effect, Teichner et al. [44] studied the properties of Pt supported over polyamide polymers (Nylon) for hydrogenation of aromatic molecules and found that the electronic enrichment of the Pt particles decreased the strength of the metal-hydrocarbon bonds thus producing a weaker adsorption.

Both the experimental data and the prediction of Model 7 are plotted in Fig. 4 to 6. Fig. 7(a) to 7(c) contain plots of the residuals of the styrene concentration for sets of runs with one varying reaction condition and all other conditions constant (variable styrene concentration, variable pressure, variable temperature). For all runs it is evident that the fitting of the model is better at the beginning of the run and at medium and long reaction times, with a slightly poorer fit at 50-150 min.

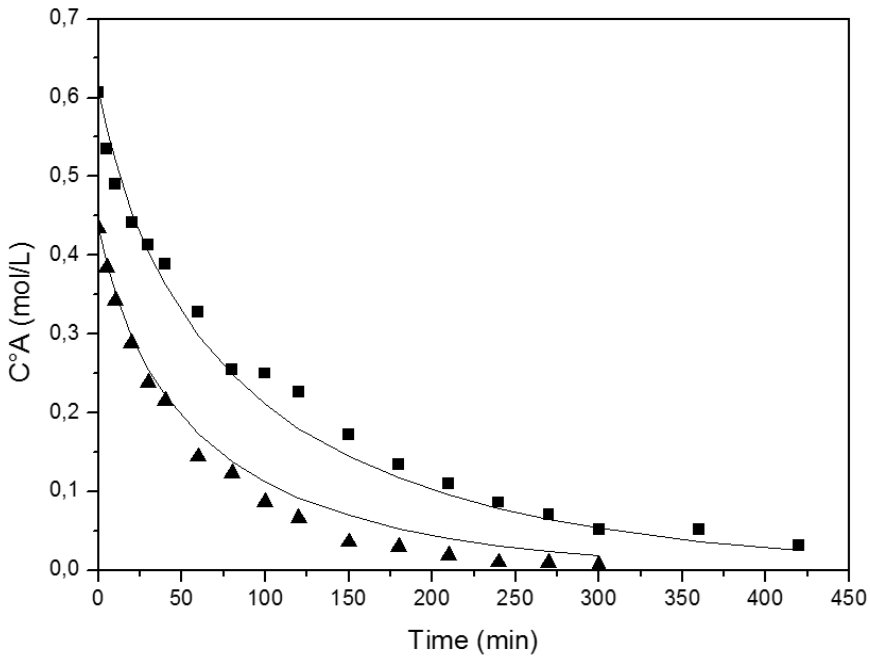

Fig. 4 Experimental data (points) and model 7 prediction (solid line). (■) P=20 bar, T=373 K, C°_{A}=0.60 M (▲) P=10 bar, T=373 K, C°_{A}=0.43 M

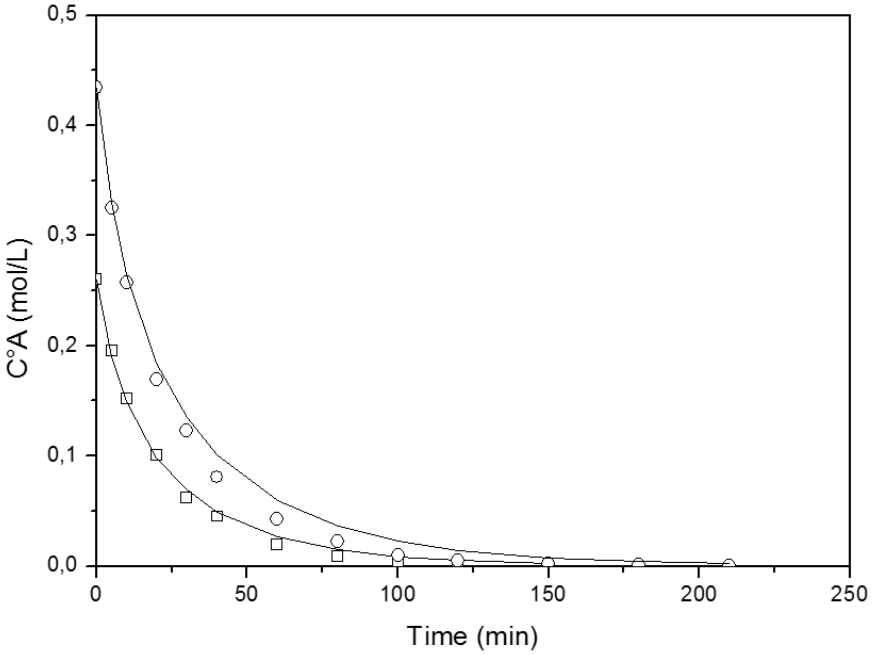

Fig. 5 Experimental data (points) and model 7 prediction (solid line). (□) P=20 bar, T=373 K, C°_{A}=0.26 M (○) P=20 bar, T=393 K, C°_{A}=0.43 M

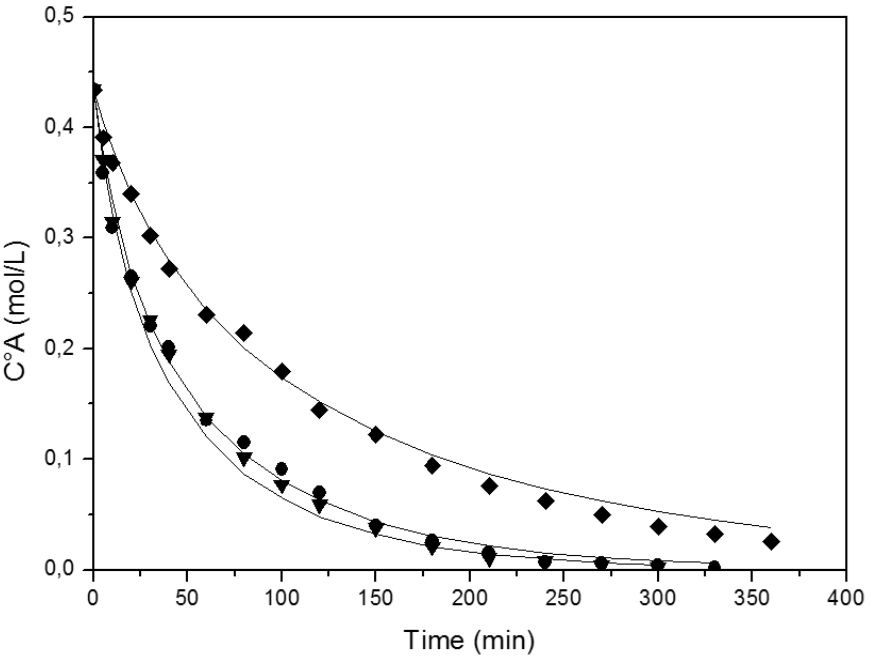

Fig. 6 Experimental data (points) and model 7 prediction (solid line). (●) P=20 bar, T=373 K, C°_{A}=0.43 M (▼) P=30 bar, T=373 K, C°_{A}=0.43 M (♦) P=20 bar, T=353 K, C°_{A}=0.43 M

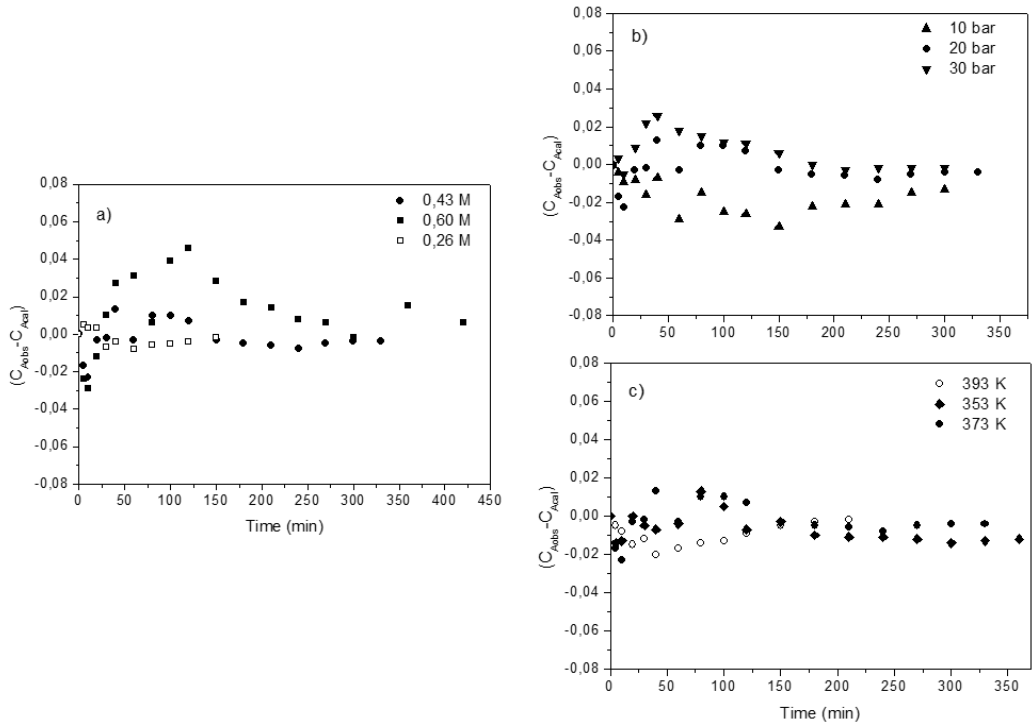

Fig. 7 Evolution of residuals for the styrene concentration. (a) P=20 bar, T=373 K, C^0_A=variable. (b) T=373 K, C^0_A=0.43 M, P=variable. (c) P=20 bar, C^0_A=0.43 M, T=variable

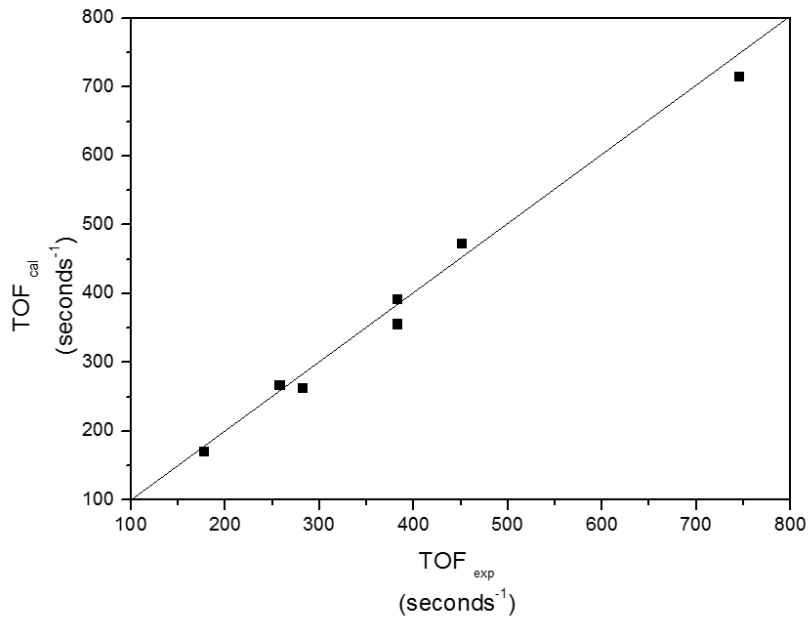

Fig. 8 Parity plot of the experimental (exp) and calculated (cal) TOF values for all runs. Calculated values correspond to those of model 7

Fig. 8 is a parity plot of the initial reaction rates: experimental compared to calculated, in terms of TOF values. For all runs the deviation is small. The maximum deviation found was 4.3%. The trend of the curve confirms the excellent fit achieved with Model 7. The parity plot also shows that the range of initial TOF values is 170-710 s^{-1} (number of molecules reacted per

unit surface Pd atom and second), a range considered normal for styrene hydrogenation over Pd at the given reaction conditions. For example Silvestre-Albero et al. report TOF values of 1.1-9.6 s^{-1} for 1,3-butadiene hydrogenation on Pd/Al_2O_3 at 373 K [45]. De Souza Monteiro et al. [46] report TOF values of 17-57 s^{-1} at 370 K for 1,3-butadiene hydrogenation over Pd/CeO_2-Al_2O_3. Corvaisier et al. [26] report a TOF of 254 s^{-1} for the hydrogenation of styrene at 373 K on a Pd/SiO_2 catalyst. Gao et al. [47] found that palladium-pyridil films are highly active catalysts for styrene hydrogenation, with TOF values of 2 s^{-1} at room temperature.

Table 8 Comparison of TOF and selectivity values of the studied catalyst and a conventional Pd catalyst. P=20 bar, T=373 K, $C°_A$=0.43 M.

Catalyst name	Pd content, mass %	TOF [(a)]	Selectivity to EB, % [(b)]
0.3PdBTAl	0.26	383	99.32
Procatalyze LD265 (Pd/Al_2O_3)	0.30	314	99.65

[(a)] TOF: reacted molecules per unit surface Pd atom and second.
[(b)] Selectivity: moles of EB * 100 / total number of moles of product. EB: ethylbenzene

Table 8 is a comparison of the activity and selectivity of 0.3PdBTAl and a commercial Pd/Al_2O_3 catalyst. It can be seen that the activity and selectivity are very similar. In both cases the only secondary product detected was ethyl cyclohexane. These similarities point to a similar mechanism being present in both Pd based catalysts, irrespective of the support. The high selectivity to EB occurs even when styrene is a minor component of a complex mixture. For example Chen et al. [48] report that during the hydrotreatment of a xylene mixture feedstock over a Procatalyze Pd/Al_2O_3 catalyst, styrene is practically fully converted to ethylbenzene.

The fact that the Horiuti-Polanyi model gave a good fit of the data for hydrogenation of the vinyllic bond could have been anticipated. Since the mechanism was first proposed in 1934 it has received a sound confirmation from other experimental works on hydrogenation of different kinds of alkenes and other double bond containing molecules [49]. The two-step hydrogen insertion, with one step being rate-limiting and the other being equilibrated has been thoroughly confirmed by experiments of deuterium exchange with different reacting systems. The presence of an ethyl intermediate (C_2H_5) during the hydrogenation of ethylene was confirmed by Somorjai and Rupprechter by using single crystal Pt catalysts and sum frequency generation vibrational spectroscopy [50]. The same authors report that for Pt(111) the adsorbed pi bonded ethylene species seems to be weakly bounded and produces most of the ethane, while ethylidyne and di-sigma bonded ethylene are spectators during the catalytic process. Despite the general acceptance of the model it has been argued that it is not entirely consistent with the observed kinetics of some systems. Some authors have pointed out that this problem can be related to the inadequacy of the Langmuir model for adsorption that is included in the Horiuti-Polanyi mechanism. Relaxation of this constraint and incorporation of a model for finite metal particle sizes, hydrogen spillover and diffusion seems to reproduce the experimental data better [51].

Regarding the rate-limiting step of the best fitting model, insertion of the first hydrogen to form the half-hydrogenated intermediate is perhaps the most common assumption found for step-wise hydrogenation of alkenes, as in the case of the report of liquid phase isooctane hydrogenation of Lylykangas et al [52]. However the second insertion is sometimes regarded as rate-limiting, as in the case of the report of Rekoske et al. [53] for hydrogenation of ethylene on Pt, or the report of Corvaisier et al. [26] for styrene hydrogenation on different transition metals. In the case of this kinetic study the error difference between models 7 and 8 (χ^2 of model 8 is about 50% higher than χ^2 of model 7) is considered big enough to rule out the possible presence of a mechanism in which the second hydrogenation step is rate-limiting.

Recalling the comparison of the apparent activation energies (Table 2) and equations (28) and (34) it could be rationalized that the apparent activation energy is related to the E_1 parameter that involves the true activation energy of the rate-limiting step, the equilibrium constant for adsorption of styrene and the equilibrium constant for dissociative chemisorption of hydrogen. Given the small value of E_a in comparison to the value of ΔH_A and especially ΔH_{H2} it can be seen that the "kinetic" apparent activation energy is greatly masked by the convolution of thermodynamic adsorption phenomena.

Finally a word should be said about the high selectivity obtained for the partial hydrogenation of styrene to ethylbenzene over this Pd/composite catalyst. No acid-catalyzed cracking or oligomerization products were found due to the low acidity of the polymeric support. Tests of acidity in the reaction of dehydration of 1,4-butanediol have indicated that these composite supports have lower acidity than activated carbon and aluminas [54]. With respect to the inhibition of the hydrogenation of the aromatic ring, selectivity can be usually modified regulating the reaction temperature, the metal loading and the electronic state of the metal. According to Corvaisier et al. [26] a great level of selectivity is obtained on any transition metal if the temperature is sufficiently low, given the greater activation energy of hydrogenation of the aromatic carbons. The authors studied the hydrogenation of styrene at 323 K and obtained 97% selectivity to ethylbenzene with Ir and Cu catalysts (3% selectivity to ethylcyclohexane) and 100% selectivity to ethylbenzene with Pd, Pt, Co, Ni, Ru and Rh. Another factor

influencing the selectivity is the metal loading. Parvulescu et al. [55] reported that supported Pd catalysts with 0.1 wt% Pd are completely selective to ethylbenzene while catalysts with 0.3-0.5 wt% Pd are not. In our case a 0.3 wt% metal loading is used and a beneficial effect related to low metal loading should not be present. Finally if we analyze the state of the metal, the electron deficiency should seemingly improve the rate of hydrogenation of the aromatic nucleus. For example Lin and Vannice [56-57] concluded that the electron deficiency enhances the activity of Pt and Pd for benzene and toluene hydrogenation. In our case no hydrogenation of the aromatic ring was observed, despite the relatively high temperature and electron deficiency of the metal function. This is in agreement with the normal behavior of alkylsubstituted rings for which hydrogenation is slower than alkene hydrogenation in the presence of noble metal catalysts at mild temperatures (lower than 400 K).

Conclusions

The kinetics of the selective hydrogenation of styrene to ethylbenzene over Pd supported on an organic-inorganic composite support was studied. The basic characterization of the catalyst shows an egg-shell distribution of metal palladium particles. The composite supported Pd particles were found to be partly electrodeficient (75.6% $Pd^{\delta+}$ with δ close to 0, 24.4% Pd^{n+}, with n close to 2) as a consequence of the interaction with residual surface chloride anions. The hydrogenation of styrene in the liquid phase over this catalyst was found to be completely selective to ethylbenzene with no products of deep hydrogenation or oligomerization.

Several models were tried against a set of data obtained at different conditions of hydrogen pressure, temperature and initial styrene concentration. The models that best fitted the data were those with the surface reaction as rate limiting step.

A 3-parameters model posing a Horiuti-Polanyi mechanism with competitive adsorption of styrene, ethylbenzene and hydrogen, and negligible concentration of free sites was found to best adjust the experimental data. The rate-limiting step was the insertion of the first hydrogen. The heats of adsorption of styrene and ethylbenzene were calculated from the kinetic results and an almost equal value of -13 kCal mol^{-1} was obtained (exothermal).

Acknowledgements

The authors are gratefully indebted to CONICET, ANPCyT and Universidad Nacional del Litoral for financially sponsoring this research work.

References

1. Guczi L, Molnár Á, Teschner D, Hydrogenation Reactions: Concepts and Practice, in "Comprehensive Inorganic Chemistry II (Second Edition). From Elements to Applications", Vol. 7, 2013, Elsevier, 421-457.
2. Molnár Á, Sárkány A, Varga M (2001) J Mol Catal A Chem 173: 185–221.
3. de Medeiros JL, Araújo OQF, Gaspar AB, Silva MAP, Britto JM (2007) Braz J Chem Eng 24:119-133.
4. Abushwireb R, Elakrami H, Emtir M (2007) Computer Aided Chemical Engineering 24:1071-1076.
5. Cole EL, Nolan JT (1995) Stabilizing Pyrolysis Naphtha, US Patent 4,009,094.
6. Badano J, Lederhos C, Quiroga M, L'Argentière P, Coloma-Pascual F (2010) Quim Nova 33:48-51.
7. L'Argentiere PC, Fígoli NS (1998) React. Kinet. Catal. Lett. 64: 221-228.
8. Badano JM, Quiroga M, Betti C, Vera C, Canavese S, Coloma-Pascual, F (2010) Catal Lett 137:35-44.
9. Badano JM, Betti C, Rintoul I, Vich-Berlanga J, Cagnola E, Torres G, Vera C, Yori J, Quiroga M (2010) Appl Catal A: General 390:166-174.
10. Badano JM, Lederhos CR, Quiroga M, L´Argentiere P, Betti C, Vera CR, Rintoul I, Gugliotta L (2009) Patent P-090103151, INPI Argentina.
11. Carrara N, Badano JM, Betti C, Lederhos C, Rintoul I, Coloma-Pascual F, Vera C (2015) Catal Comm 61:72-77.
12. Papp A, Miklós K, Forgo P, Molnár A (2005) J Mol Catal A Chem 229:107–116.
13. Lederhos CR, L'Argentiere PC, Coloma-Pascual F, Fígoli NS (2006) Catal Lett 110:23-28.
14. Dormand JR, Prince PJ (1980) J Comp Appl Math 6:19-26.
15. Byrd RH, Gilbert JC, Nocedal J (2000) J Mathematical Programming 89:149-185.
16. Lagarias JC, Reeds JA, Wright MH, Wright PE (1998) SIAM Journal on Optimization 9:112-147.
17. Carruth GF, Kobayashi R (1973) J Chem Eng 18:115-126.
18. Abo-Ghander NS, Logist F, Grace JR, Van Impe JF, Elnashaie SSEH, Lim CJ (2014) Chemical Engineering and Processing: Process Intensification 77:50–65.
19. Asatani H (1986) Solubility of gases in liquids, Doctoral Thesis, University of Ottawa.

20. Carrara N, Badano J, Bertero N, Torres G, Betti C, Martinez-Bovier L, Quiroga M, Vera C (2014) J Chem Technol Biotechnol 89:265-275.
21. L'Argentière PC, Fígoli NS, Arcoya A, Seoane XL (1991) React. Kinet. Catal. Lett. 43: 413-417.
22. Bozon-Verduraz F, Omar A, Escard J, Pontvianne B (1978) J Catal 53:126-134.
23. Fígoli NS, L'Argentiere PC, Arcoya A, Seoane XL (1995) J Catal 155:95-105.
24. Gaspar AB, dos Santos GR, de Souza-Costa R, da Silva MAP (2008) Catal Today 133:400-405.
25. Smith JM (1970) Chemical Engineering Kinetics, McGraw-Hill: New York.
26. Corvaisier F, Schuurman Y, Fecant A, Thomazeau C, Raybaud P, Toulhoat H, Farrusseng D (2012) J Catal 307:352-361.
27. Cheng YM, Chang JR, Wu JC (1986) Appl Catal A: General 24:273-285.
28. Kacer P, Cervený L (2004) J Mol Catal A Chem 212:183-189.
29. Zhou Z, Cheng Z, Cao Y, Zhang J, Yang D, Yuan W (2007) Chem Eng Technol 30:105-111.
30. Jackson SD, Shaw LA (1996) Appl Catal A: General 134:91-99.
31. Nijhuis TA, Dautzenberg FM, Moulijn JA (2003) Chem Eng Sci 58:1113-1124.
32. Ali J (2012) The hydrogenation of pyrolysis gasoline (PyGas) over nickel and palladium catalysts, Doctoral Thesis, University of Glasgow.
33. Chou P, Vannice MA (1987) J Catal 107:129-139.
34. Tsuchiya S, Amenomiya Y, Cvetanovic RJ (1970) J Catal 19:245-255.
35. Horiuti J, Polanyi M (1934) Trans Faraday Soc 30:1164-1172.
36. Gallezot P (2003) In: Encyclopedia of Catalysis, Hydrogenation – Heterogeneous, Horvath IT, John Wiley & Sons.
37. Conrad HH, Ertl G, Latta EE (1974) Surf Sci 41:435-446.
38. Zhou Z, Zeng T, Cheng Z, Yuan C (2010) Chem Eng Sci 65:1831-1839.
39. Ranke W, Joseph Y (2002) Phys Chem Chem Phys 4:2483-2498.
40. Smeds S, Murzin D, Salmi T (1995) Appl Catal A: General 125:271-291.
41. Chaudhari RV, Jaganathan R, Kolhe DS, Emig G, Hofmann H (1986) Chem Eng Sci 41:3073-3081.
42. Singh UK, Vannice MA (2001) Appl Catal A: General 213:1-24.
43. Bond G (2005) In: Metal catalyzed reactions of hydrocarbons, Springer Science, New York.
44. Teichner SJ, Hoang-Van C, Astier M (1982) Stud Surf Sci Catal 11:121-140.
45. Silvestre-Albero JS, Rupprechter G, Freund HJ (2006) J Catal 240: 58-65.
46. De Souza Monteiro R, Bellot Noronha F, Chaloub Dieguez L, Schmal M (1995) Appl Catal A: General 131: 89-106.
47. Gao S, Li W, Cao R (2015) J Coll Interf Sci 441: 85-89.
48 Chen TJ, Ou JDY, Abichandani JS, Heeter GA, US Patent Application 0221710 (2014).
49. Mattson B, Foster W, Greimann J, Hoette T, Le N, Mirich A, Wankum S, Cabri A, Reichenbacher C, Schwanke E (2013) J Chem Educ 90:613-619.
50. Somorjai GA, Rupprechter G, In: Dynamics of Surfaces and Reaction Kinetics in Heterogeneous Catalysis, Froment GF, Waughan KC (1997) Elsevier.
51. Jackson SD, Hargreaves JSJ, Lennon JD (2003) Catalysis in Application, Royal Society of Chemistry, Cambridge.
52. Lylykangas MS, Rautanen PA, Krause AOI (2003) AIChE Journal 49:1508-1515.
53. Rekoske JE, Cortright RD, Goddard SA, Sharma SB, Dumesic JA (1992) J Phys Chem 96:1880-1880.
54. Badano J (2008) Doctoral Thesis, Universidad Nacional del Litoral, Argentina.
55. Parvulescu VI, Filoti G, Parvulescu V, Grecu N, Angelescu E, Nicolescu IV (1994) J Mol Catal 89:267-282.
56. Lin SD, Vannice MA (1993) J Catal 143:539-553.
57. Lin SD, Vannice, MA (1993) J Catal 143:554-562.